Available online at www.sciencedirect.com
ScienceDirect
Journal of Power Sources 161 (2006) 1392–1399
JOURNAL OF POWER SOURCES
www.elsevier.com/locate/jpowsour

Evaluation of the electrochemical stability of graphite foams as current collectors for lead acid batteries

Young-Il. Jang [a], Nancy J. Dudney [a,*], Terry N. Tiegs [b], James W. Klett [b]

[a] *Condensed Matter Sciences Division, Oak Ridge National Laboratory, Building 3025, MS 6030, P.O. Box 2008, Oak Ridge, TN 37831, USA*
[b] *Metals and Ceramics Division, Oak Ridge National Laboratory, Oak Ridge, TN 37831, USA*

Received 23 February 2006; received in revised form 25 April 2006; accepted 27 April 2006
Available online 9 June 2006

Abstract

Graphite foams with high electrical and thermal conductivities, good mechanical strength, and low mass have been synthesized and evaluated as possible current collector materials to replace lead alloys for the development of lightweight lead acid batteries. Cyclic voltammetry and galvanostatic charge–discharge tests were performed on these foams prior to and after graphitization to evaluate their electrochemical properties. In the voltage range where the negative electrode of lead acid batteries operates, the graphite foam is electrochemically stable. However, in the voltage range of the positive electrode, the graphite foam is not electrochemically stable due to intercalation of sulfuric acid into graphite. For the positive electrode, the non-graphitized foam shows better electrochemical stability and warrants further study for use as a current collector. Preliminary charge/discharge characterization of these graphite and non-graphitized foams coated with a lead oxide battery paste supports these conclusions, although the paste formulation and coating process need to be improved for cycle life evaluation.
Published by Elsevier B.V.

Keywords: Carbon foam; Graphite foam; Lead acid battery; Current collector; Cyclic voltammetry; Intercalation

1. Introduction

A variety of battery chemistries are being researched as the demand for smaller, lighter, and longer life power sources expands. Although newer battery chemistries, including various lithium, lithium-ion, and nickel metal hydride batteries, achieve specific energies and energy densities significantly greater than that of the lead acid batteries, advanced lead acid batteries are still one of the most reliable, economical, and environmentally friendly options. The biggest drawback of lead acid batteries is the heavy weight due to the use of lead as the current collector material. Lead grids constitute 20–30% of the battery weight. To reduce the dead weight of lead acid batteries, lightweight, electronically conducting materials based on carbon are widely investigated as potential substitutes for the lead current collectors [1–6]. Previous works on reticulated vitreous carbon (RVC), which is an open-pore foam of glass-like carbon, indicated that carbon foams are promising as a current collector material for the development of lower weight lead acid batteries [2,3,5–7]. Furthermore, it has been shown that high specific surface area current collectors such as carbon foam improve the utilization efficiency of the paste material due to the higher interface area and thinner paste coating [5,6,8]. While the use of RVC as battery current collectors was first proposed more than a decade ago, lead acid batteries employing RVC current collectors are still at the development stage [9]. A possible reason for the delay in their commercialization is the softness of RVC (ultimate compressive strength: 763 kPa at 20 °C), as the electrical and thermal conductivities (1.3 S cm^{-1}, 0.085 W m^{-1} K^{-1}) may be adequate [10].

Recently, new graphite foams were developed at Oak Ridge National Laboratory (ORNL) [11,12]. Among other applications, the notion of using these graphite foams as current collectors for lead acid batteries has been proposed and documented in a recent patent application [13]. Unfortunately, no experimental battery results are provided. The ORNL graphite foams have a number of attractive properties. They are lightweight (0.6 g cm^{-3}) and chemically inert with many acids. The surface area is ca. 200 cm^2 cm^{-3}. The conductive graphene planes are oriented along the walls of the foam, giving the monolithic struc-

* Corresponding author. Tel.: +1 865 576 4874; fax: +1 865 574 4143.
E-mail address: dudneynj@ornl.gov (N.J. Dudney).

0378-7753/$ – see front matter. Published by Elsevier B.V.
doi:10.1016/j.jpowsour.2006.04.124

ture very high electrical and thermal conductivities (10^3 S cm^{-1}, 180 W m^{-1} K^{-1}) [14], significantly higher than those of RVC. The excellent transport properties may help ensure a uniform current distribution in the battery electrode, which is important to achieve maximum energy and lifetimes. Furthermore, the compressive strength of graphite foam is 2.1–5.1 MPa, higher than that of RVC by an order of magnitude. The combination of physical properties may improve both the manufacturability and performance of lead acid batteries when the graphite foams are used as current collectors. Further, the physicochemical properties of foam current collectors, including the density and pore size, can be tuned by choosing different precursors, synthesis pressure and temperature, heat rates, and additives. Here, we report electrochemical properties of the ORNL graphite foams when tested as the bare foams in sulfuric acid and also in preliminary tests of the foams coated with a lead oxide paste to evaluate a complete battery electrode.

2. Experimental

The foams used in this study are the same as the ORNL graphite foams described above. They were synthesized from Mitsubishi ARA24, which is a mesophase, naphthalene-based synthetic pitch. The foam structure was produced by heating the pitch in an aluminum pan at 1 °C m^{-1} under 1000 psi pressure and were fully carbonized upon 1000 °C. This process produced foams with a density of about 0.55 g cm^{-3}, a pore size of about 300 μm, and windows between the pores of about 100 μm. Foams processed to this extent are referred to as "non-graphitized." A further heat treatment to 2800 °C in argon is needed to graphitize the foam. The graphitized material has graphene sheets well-aligned along the pore walls giving exceptionally high thermal and electrical conductivities. Four point conductivity measurements of the graphitized and non-graphitized foams used in this study gave conductivities of 300 and 40 S cm^{-1}, respectively. While the non-graphitized foam has a lower conductivity than graphite foam, its conductivity is approximately 30 times higher than that of RVC (1.3 S cm^{-1}).

The foams used for electrochemical tests were cut from larger billets into coupons approximately 25 mm × 12.5 mm × 2.5 mm. Electrical connection between the carbon foams and electrical lead wires was made by mechanical pressure using metallic alligator clips coated with a corrosion-resistant polymer resin. Electrochemical characterizations were performed using three-electrode beaker cells. In all cases, the reference electrode was Hg/Hg_2SO_4 in saturated K_2SO_4 solution (MSE), and 50 mL of H_2SO_4 solution in various concentrations was used as the electrolyte. The electrolyte was not stirred during the electrochemical test. The counter electrodes were either large pieces of graphite foam or 0.125-in. diameter lead wire.

Cyclic voltammetry was performed at a scan rate of 5 mV s^{-1} using a Solartron 1286 potentiostat/galvanostat controlled by CorrWare software running on a PC. The foam pieces cut for the working electrodes were ca. 0.1 g. For comparison, cyclic voltammetry was also performed on a metallic lead wire, with a geometrical area immersed in the electrolyte of ca. 2 cm^2, and also on foams coated with ca. 0.4 or 0.9 g of the lead oxide paste described below. Unless otherwise stated, the test results presented were initiated at the open circuit cell potential.

The battery pastes were made using a process found in the patent literature [15]. The procedure involves combining powders of PbO (50 g, Alfa Aesar, 99.9%, −325 mesh), Pb (16.6 g, Alfa Aesar, 99%, −200 mesh) and Pb_3O_4 (16.6 g, Alfa Aesar, 97%, −325 mesh). This mixture of metallic and oxide powders was combined with a solution of distilled water (20.2 g) and teflon (1.4 g, Dupont, TFE 30) to make a paste. Sulfuric acid (5.5 g of 50% solution) was then added in small amounts with stirring. After about 5 min, additional water (11 g) was added to adjust the viscosity. The pastes were then physically forced into the pores of the ca. 2.5 mm-thick foam coupons with a spatula, and excess paste was scraped off of the surface. The pasted foams were cured at ca. 65 °C for >12 h. By X-ray diffraction, the prepared electrodes were largely β-PbO and $3PbO{\cdot}PbSO_4{\cdot}H_2O$. Subsequent examination of the electrodes showed that the paste was largely at the outer surfaces and did not completely penetrate the foam. It is clear that the paste formulation and the coating technique need to be refined to achieve a uniformly coated electrode structure. This is left to future work. Fig. 1 shows a scanning electron microscope image of lead oxide paste coated graphite foam. Lead oxide paste of 100–300 μm in thickness is coated on the surface of the foam.

With the pasted electrodes, galvanostatic charge–discharge was performed on three-electrode beaker cells at 10 mA (*C*/20) using a Maccor 4000 series battery test system. Carbon foams coated with lead oxide paste were used as both positive and negative electrodes, and MSE as the reference electrode. Flooded cells were used with no separator material between the plates. The amount of lead oxide active material coated on the foam was ca. 0.9 g, giving a theoretical capacity of about 230 mAh. During charge and discharge, potentials of the positive and negative electrodes with respect to the reference electrode were measured in addition to the overall cell voltage. After the electrochemi-

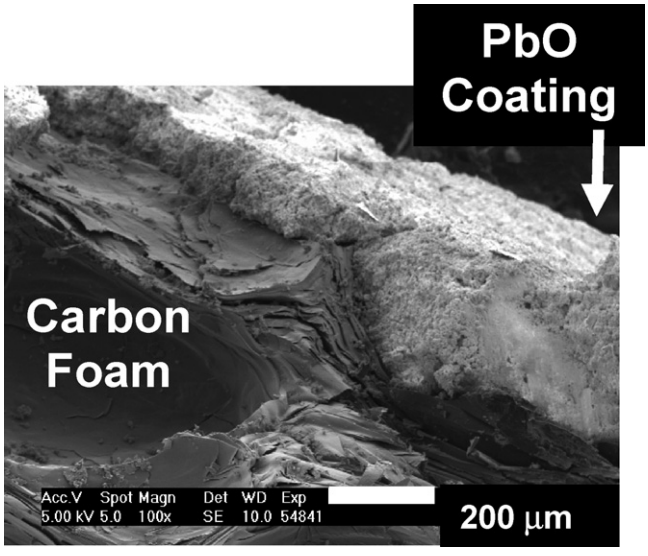

Fig. 1. Scanning electron microscope (SEM) image of lead oxide paste coated on graphite foam.

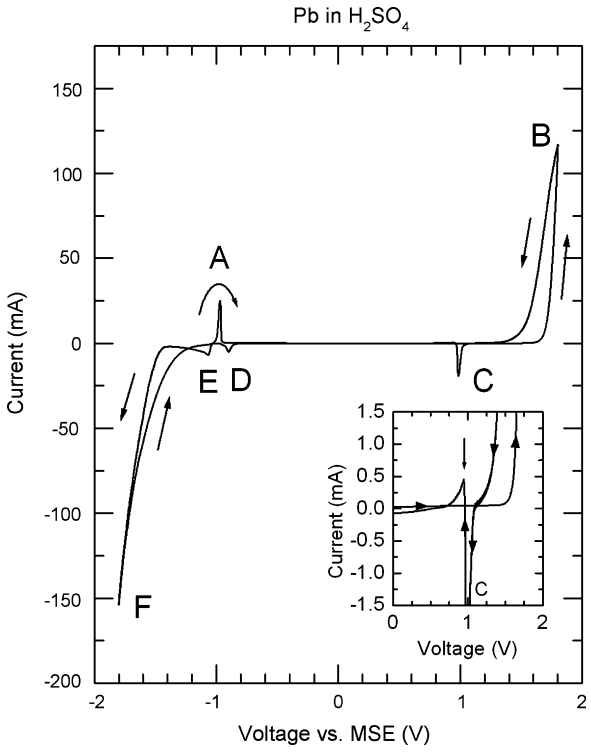

Fig. 2. Cyclic voltammogram of metallic lead between −1.8 and 1.8 V vs. Hg/Hg_2SO_4 in saturated K_2SO_4 solution. The scan rate is 5 mV s^{-1}, and the electrolyte is 4.5 M H_2SO_4 solution. See the text for the redox reactions corresponding to the peaks A–F.

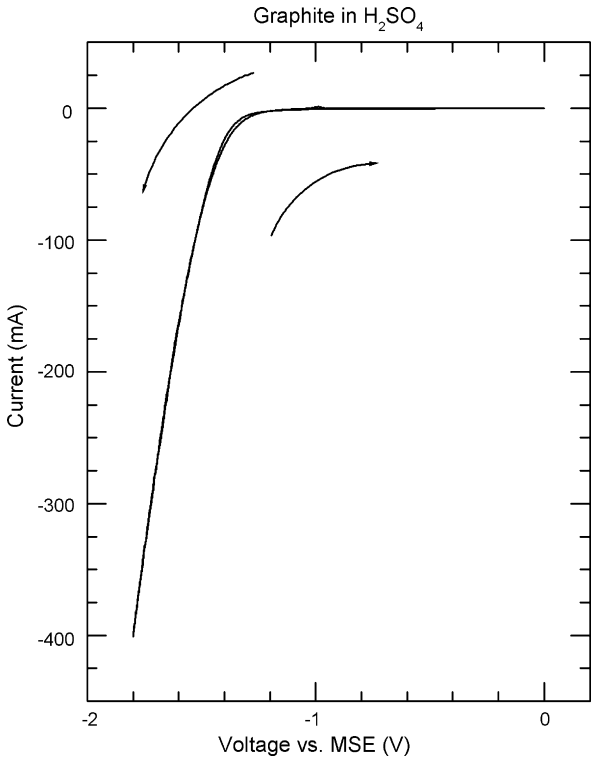

Fig. 3. Cyclic voltammogram of graphite foam between −1.8 and 0 V vs. Hg/Hg_2SO_4 in saturated K_2SO_4 solution. The scan rate is 5 mV s^{-1}, and the electrolyte is 4.5 M H_2SO_4 solution.

cal tests, X-ray diffraction (XRD) was performed on the intact electrodes using Cu Kα radiation (Scintag XDS 2000).

3. Results and discussion

Fig. 2 shows a typical cyclic voltammogram of metallic lead between −1.8 and 1.8 V versus MSE in 4.5 M H_2SO_4 solution. The main redox processes of the lead electrode indicated by peaks A–F are as follows: (A) $Pb \rightarrow PbSO_4$; (B) $PbSO_4 \rightarrow PbO_2$ and O_2 evolution; (C) $PbO_2 \rightarrow PbSO_4$; (D) $PbO \rightarrow Pb$; (E) $PbSO_4 \rightarrow Pb$; (F) H_2 evolution [16]. The peaks are related to half-cell reactions occurring in lead acid batteries during charge and discharge, as summarized in Table 1. Positive hysteresis associated with peak B is noticeable, i.e. currents recorded on the cathodic scan are greater than those recorded on the anodic scan. This is explained in terms of the large nucleation overpotential required to initiate the growth of PbO_2 nuclei in the polycrystalline layer of $PbSO_4$ formed earlier in the anodic scan [16]. The reduction of PbO_2 to $PbSO_4$ at peak C is accompanied by a large increase of the molar volume. As a result, the sulfate layer cracks, exposing bare metallic lead. A small oxidation peak is observed after the main reduction peak C (see arrow in the inset). This peak is due to oxidation of freshly exposed Pb to $PbSO_4$ [17]. Fig. 2 will be compared with cyclic voltammograms obtained from graphite foam coated with lead oxide paste (see below).

Fig. 3 shows a cyclic voltammogram of a graphite foam working electrode between −1.8 and 0 V versus MSE in 4.5 M H_2SO_4 solution. No feature is observed in this voltage range except the onset of hydrogen evolution at −1.2 V. This indicates that the graphite foam is electrochemically stable between −1.2 and 0 V. Since the redox reactions at the negative electrode of lead acid batteries occur above −1.2 V versus MSE, as indicated by the

Table 1
Half-cell reactions during charge and discharge of lead acid batteries corresponding to the redox peaks A–F observed in cyclic voltammogram of metallic lead (Fig. 2)

Peak	Reaction	Potential (V) (vs. Hg/Hg_2SO_4)	Electrode	Charge/discharge
A	$Pb + SO_4^{2-} \rightarrow PbSO_4 + 2e^-$	−1.0	Negative	Discharge
B	$PbSO_4 + 2H_2O \rightarrow PbO_2 + H_2SO_4 + 2H^+ + 2e^-$	>1.3	Positive	Charge
	$H_2O \rightarrow \frac{1}{2}O_2 + 2H^+ + 2e^-$		Positive	Overcharge
C	$PbO_2 + H_2SO_4 + 2H^+ + 2e^- \rightarrow PbSO_4 + 2H_2O$	1.0	Positive	Discharge
D	$PbO + 2H^+ + 2e^- \rightarrow Pb + H_2O$	−0.9	N/A	N/A
E	$PbSO_4 + 2e^- \rightarrow Pb + SO_4^{2-}$	−1.1	Negative	Charge
F	$2H^+ + 2e^- \rightarrow H_2$	<−1.44	Negative	Overcharge

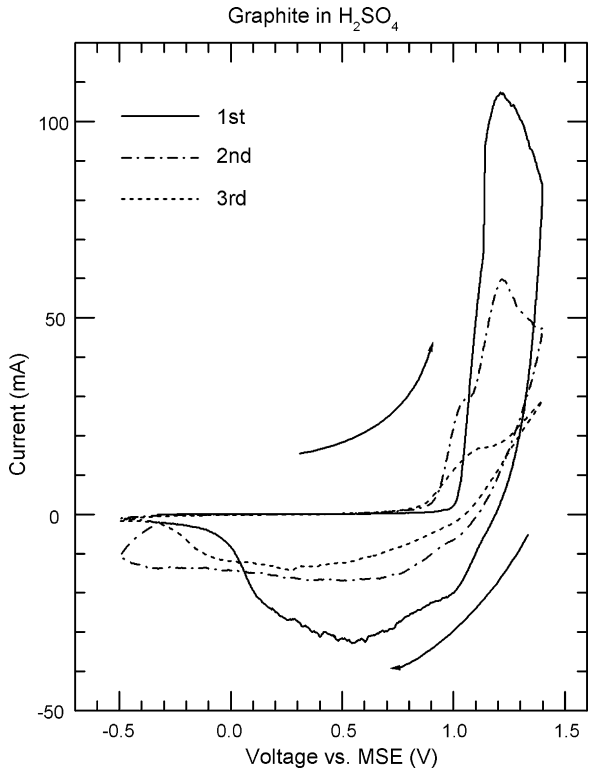

Fig. 4. Cyclic voltammogram of graphite foam between −0.5 and 1.4 V vs. Hg/Hg_2SO_4 in saturated K_2SO_4 solution. The scan rate is 5 mV s^{-1}, and the electrolyte is 4.5 M H_2SO_4 solution.

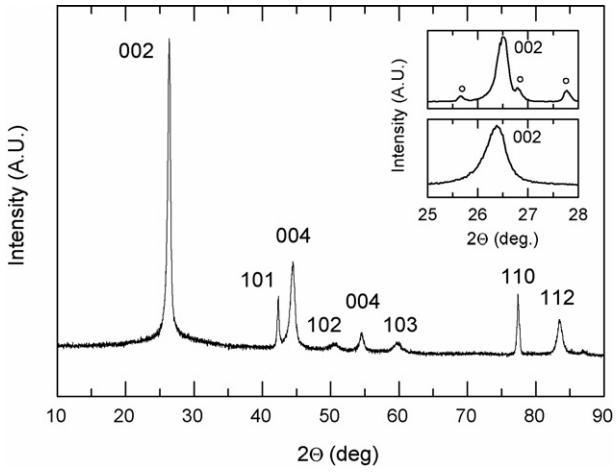

Fig. 5. X-ray diffraction pattern of graphite foam after cyclic voltammetry experiments (five cycles between −0.5 and 1.4 V vs. MSE). Miller indices (*h k l*) are indexed based on the space group $P6_3/mmc$. The upper inset shows the (0 0 2) peak from an uncycled graphite foam coated with lead oxide paste after storage in 4.5 M H_2SO_4 solution for 12 hrs, compared to the (0 0 2) peak from the cycled graphite foam (◯: $PbSO_4$, JCPDS #36-1461).

peaks A and E in Fig. 2, graphite foam is suitable for use as negative current collector. Combined with their excellent transport properties, low mass density, and high surface area, the electrochemical stability in this voltage range makes *graphite foams a promising candidate for negative current collector*.

Fig. 4 shows typical cyclic voltammograms of a graphite foam between −0.5 and 1.4 V versus MSE in 4.5 M H_2SO_4 solution. For the first cycle, broad peaks are seen at 1.2 and 0.5 V during anodic and cathodic scans, respectively. These peaks are attributed to intercalation and deintercalation of sulfuric acid into graphite, respectively. Subsequent cycles showed somewhat smaller peaks. It is well known that graphite is electrochemically oxidized in a concentrated sulfuric acid to form graphite–sulfuric acid intercalation compounds as follows: $C_x + 3H_2SO_4 \rightarrow C_x{}^+HSO_4{}^- \cdot 2H_2SO_4 + H^+ + e^-$ [18,19]. A bisulfate ion and sulfuric acid molecules are inserted between graphite layers. Intercalation occurs in the anodic process, and deintercalation in the cathodic process. Material loss as a result of these intercalation reactions was evidenced by shedding of carbon particles off the foam.

Fig. 5 shows XRD pattern obtained from graphite foam immediately after the cyclic voltammetry experiments (five cycles between −0.5 and 1.4 V versus MSE). Miller indices (*h k l*) are indexed for the hexagonal phase (space group $P6_3/mmc$). The insets compare the (0 0 2) peak of the cycled graphite foam (lower inset) with that obtained from an uncycled graphite foam soaked in 4.5 M H_2SO_4 solution for 12 h (upper inset). Shift and broadening of the (0 0 2) peak is noticeable in the XRD pattern of cycled foam. The peak shift toward lower 2θ angles is attributed to the increase of the *c* spacing of the graphene planes as a result of intercalation of sulfuric acid [19], and the peak broadening to the accompanying strain in the lattice.

For the positive electrode of lead acid batteries, the oxidation of $PbSO_4$ to PbO_2 occurs at ≥1.3 V versus MSE, as indicated by the peak B in Fig. 2, so the positive current collector should be electrochemically stable at least up to 1.3 V. However, the graphite foam tested in this study is oxidized (i.e. sulfuric acid intercalation) at 1.2 V (see Fig. 4). It must be concluded that *graphite foam is not suitable for use as positive current collector* for lead acid batteries under the present experimental conditions. This is true even with less concentrated electrolyte solutions. Fig. 6 shows that the intercalation of sulfuric acid into graphite foam occurs in 2.6 and 1.3 M H_2SO_4 as well. It is interesting to note that the deintercalation potential during the cathodic scan increases with decreasing concentration.

Modification of the physical and/or chemical properties of the graphite foam is clearly necessary to enhance the electrochemical stability for use as positive current collector. It is well understood that the extent of intercalation reactions depends on the graphite or carbon lattice structure. To study the effect of crystallinity of graphite foams on the intercalation properties, we performed cyclic voltammetry on non-graphatized foams that have a similar microstructure and density to that of the graphitized foams. Fig. 7 shows the XRD pattern of non-graphitized carbon foam. Very broad peaks are observed at 2θ ∼25.5°, 43°, and 78.5°, corresponding to graphite (0 0 2), (1 0 1), and (1 1 0) peaks, respectively. The crystallite size calculated from the peak at 2θ ∼43° using the Scherrer formula [20] is 2 nm. Fig. 8 shows a typical cyclic voltammogram of this nanocrystalline foam between 0 and 1.4 V versus MSE, and the inset compares it with that of graphite foam. A 1.3 M H_2SO_4 solution was used as the electrolyte. The peaks associated with intercalation of

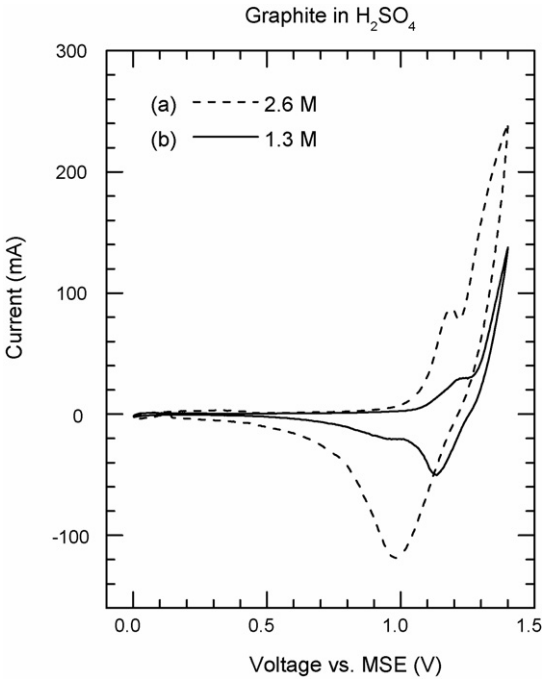

Fig. 6. Cyclic voltammogram of graphite foam between 0 and 1.4 V vs. Hg/Hg_2SO_4 in saturated K_2SO_4 solution. The scan rate is 5 mV s^{-1}, and the electrolyte is (a) 2.6 and (b) 1.3 M H_2SO_4 solution.

sulfuric acid are not observed in the non-graphitized foam, indicating that non-graphitized foams is electrochemically stable in the voltage range where the positive electrode of lead acid batteries operates. These results suggest that *non-graphitized foams could perform well as positive current collectors*.

The remaining figures show results for the graphite and non-graphitized foams coated with lead oxide paste electrodes. Although the quality of the paste coating was inadequate for good cycling performance, the cyclic voltametry, galvanic charge/discharge tests, and especially the XRD results all provide additional evidence as to whether these materials are suitable for the lead-acid battery application.

Fig. 9 shows a cyclic voltammogram between −1.8 and 0.5 V versus MSE obtained in 4.5 M H_2SO_4 solution from a

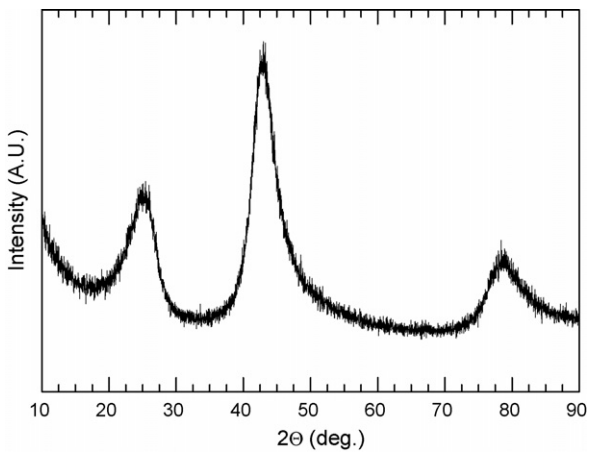

Fig. 7. X-ray diffraction pattern of non-graphitized foam.

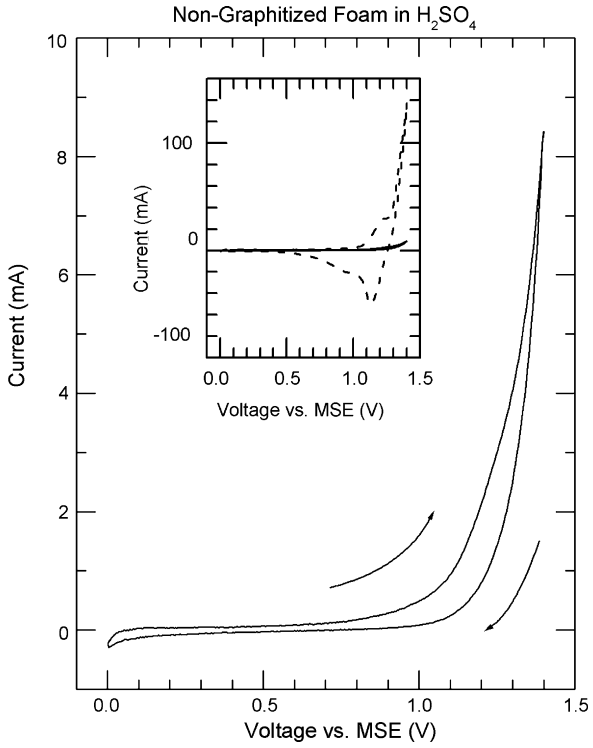

Fig. 8. Cyclic voltammogram of non-graphitized foam in H_2SO_4 between 0 and 1.4 V vs. Hg/Hg_2SO_4 in saturated K_2SO_4 solution. The inset compares cyclic voltammograms obtained from non-graphitized foam (solid line) and graphite foam (dashed line). The scan rate is 5 mV s^{-1}, and the electrolyte is 1.3 M H_2SO_4 solution.

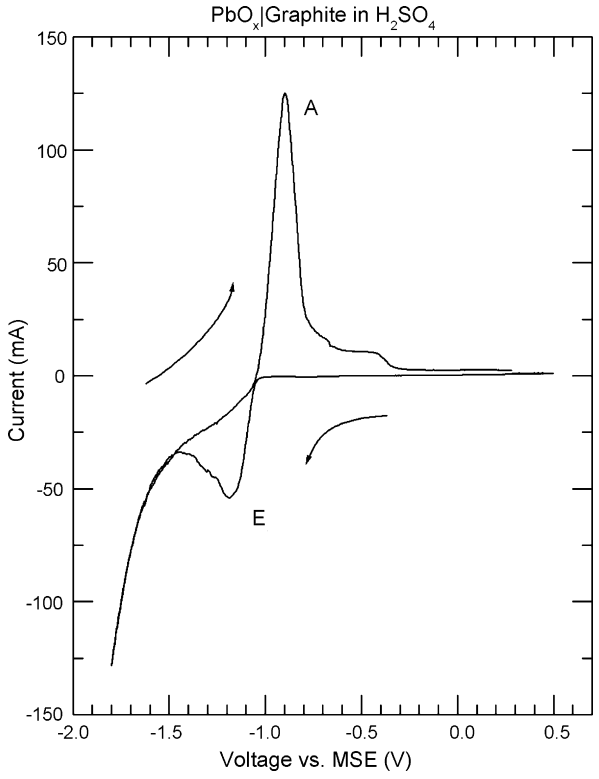

Fig. 9. Cyclic voltammogram of graphite foam coated with lead oxide paste between −1.8 and 0.5 V vs. Hg/Hg_2SO_4 in saturated K_2SO_4 solution. The scan rate is 5 mV s^{-1}, and the electrolyte is 4.5 M H_2SO_4 solution.

graphite foam coupon coated with lead oxide paste. This voltage range includes the operation voltage for the negative electrode of lead acid batteries. The cyclic voltammogram beginning at the open circuit potential was recorded right after the electrodes were put into the electrolyte, thus chemical and electrochemical changes were minimal before cyclic voltammetry. An anodic peak A and a cathodic peak E are clearly observed in Fig. 9. These are the characteristic peaks associated with the redox reaction at the negative electrode of lead acid batteries ($Pb + H_2SO_4 \leftrightarrow PbSO_4 + 2H^+ + 2e^-$) (compare with Fig. 2). The peak A corresponds to the oxidation of Pb to $PbSO_4$ (discharge), and the peak E corresponds to the reduction of $PbSO_4$ to Pb (charge) in the negative electrode. These results indicate that the electrochemical behavior of graphite foam coated with lead oxide paste resembles that of metallic lead when the oxide is reduced. Therefore, this again indicates that graphite foam is suitable for use as negative current collector.

Fig. 10 shows a typical cyclic voltammogram of a graphite foam coated with lead oxide paste between 0 and 1.5 V versus MSE in 4.5 M H_2SO_4 solution. This voltage range includes operation voltage for the positive electrode of lead acid batteries. Fig. 10 resembles Fig. 4, indicating that the intercalation of sulfuric acid into graphite is the major reaction occurring in this voltage range. Positive hysteresis associated with the $PbSO_4 \rightarrow PbO_2$ transformation is not observed. This result support the above conclusion that graphite foam is not suitable for use as positive current collector for lead acid batteries under the present experimental conditions.

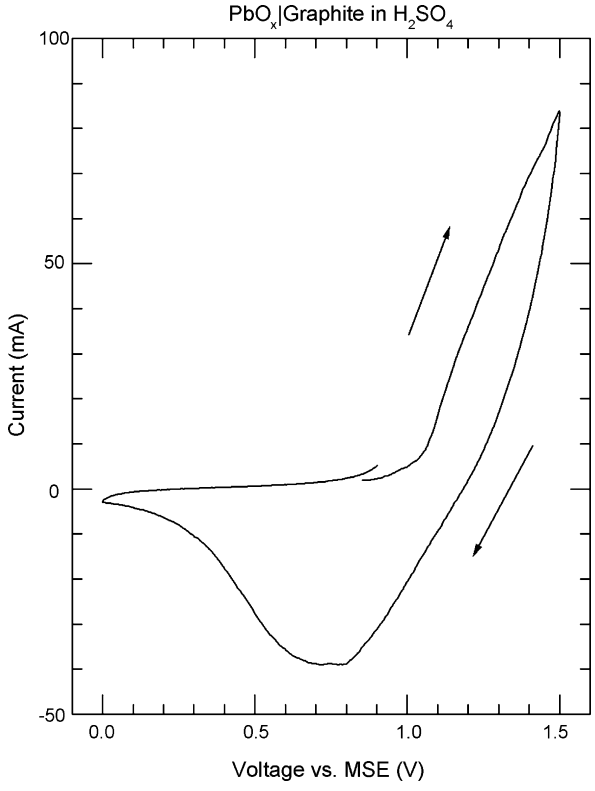

Fig. 10. Cyclic voltammogram of graphite foam coated with lead oxide paste between 0 and 1.5 V vs. Hg/Hg_2SO_4 in saturated K_2SO_4 solution. The scan rate is 5 mV s^{-1}, and the electrolyte is 4.5 M H_2SO_4 solution.

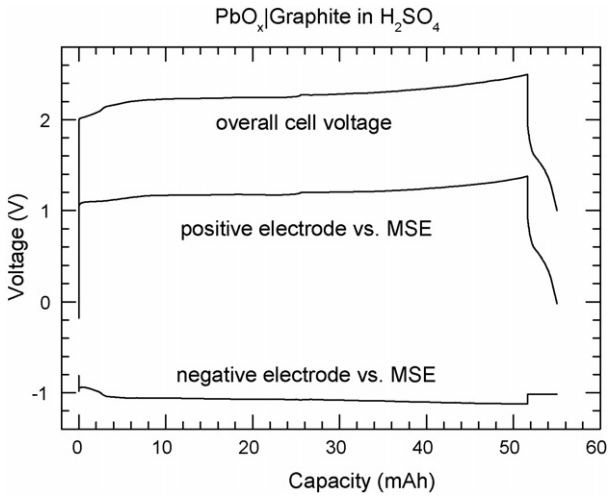

Fig. 11. First charge–discharge curves of a three-electrode cell. The positive and negative electrodes are graphite foams coated with lead oxide paste, and the reference electrode is Hg/Hg_2SO_4 in saturated K_2SO_4 solution. The charge–discharge current is 10 mA, and the electrolyte is 4.5 M H_2SO_4 solution.

Galvanostatic charge–discharge experiment was performed at 10 mA on a three-electrode cell. A 4.5 M H_2SO_4 solution was used as the electrolyte. The overall cell voltage was measured between the positive and negative electrodes, while the respective potentials of positive and negative electrodes with respect to the MSE reference electrode were simultaneously measured. Fig. 11 shows the first charge–discharge curves. The cell was initially charged to 2.5 V, and then discharged to 1.0 V. The charge–discharge curves are consistent with the cyclic voltammograms in Figs. 9 and 10. Charge and discharge of the negative electrode occurs at ca. −1 V, corresponding to the $Pb + H_2SO_4 \leftrightarrow PbSO_4 + 2H^+ + 2e^-$ reaction, while charge and discharge of the positive electrode is attributed to the oxidation and reduction of graphite foam, i.e. intercalation and deintercalation of sulfuric acid, respectively. Fig. 11 clearly shows that discharge of the cell was limited by the positive electrode, and not by the negative electrode. The cathode is clearly very resistive, and unfortunately the cell failed after the first cycle. Failure is most likely due to loss of adhesion between the lead paste and the positive current collector. Shedding of the paste from the positive electrode was observed as a result of the cycling.

Figs. 12 and 13 shows XRD patterns obtained from the negative and positive electrodes, respectively, after the galvanostatic charge–discharge. Reflections from metallic lead are clearly observed in the negative electrode, marked by black circles (JCPDS #04-0686). This indicates that the charge reaction at −1 V in the negative electrode is the reduction of $PbSO_4$ to Pb. Diffraction peaks from PbO_2 are not detected in the positive electrode, indicating that the oxidation of $PbSO_4$ to PbO_2 did not occur during charge of the positive electrode. The graphite (0 0 2) peak is indexed, and all other peaks are from $PbSO_4$ (JCPDS #36-1461).

Moving now to electrodes with the non-graphitized foam current collectors, Fig. 14 shows a typical cyclic voltammogram of a non-graphitized foam coated with lead oxide paste tested

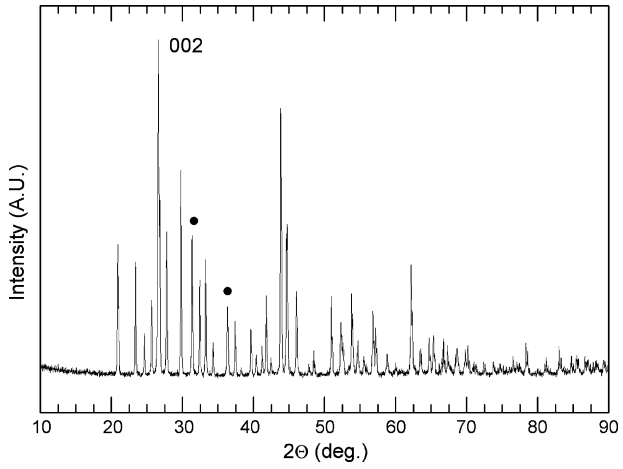

Fig. 12. X-ray diffraction pattern of graphite foam coated with lead oxide paste used as the negative electrode for a galvanostatic charge and discharge cycle between 1.0 and 2.5 V (*h k l*: graphite; ● Pb; unindexed: $PbSO_4$).

in 1.3 M H_2SO_4 solution. Positive hysteresis associated with the $PbSO_4 \rightarrow PbO_2$ transformation is clearly seen. The broad cathodic peak at 0.85 V corresponds to the $PbO_2 \rightarrow PbSO_4$ transformation (compare with Fig. 2). Fig. 15 shows galvanostatic charge–discharge curves of a three-electrode cell cycled at 10 mA between 1.0 and 2.3 V in 1.3 M H_2SO_4 solution. From the weight of active material coated on the foam, the theoretical capacity is about 230 mAh. The current density corresponds to *C*/20 rate. Very different from results for the graphitized foam of Fig. 11, the positive electrode with the non-graphitized foam (Fig. 15) shows the charge (1.1 V) and discharge (1.0 V) attributable to the $PbSO_4 \leftrightarrow PbO_2$ transformation. This is confirmed by the XRD pattern in Fig. 16 obtained from the positive electrode in the charged state after the galvanostatic cycling. Reflections from β-PbO_2 (tetragonal, JCPDS #41-1492) are clearly observed as the predominant phase.

Unfortunately, the cycle performance of this battery is still very poor. The formation of barrier layers, corrosion layers, and shedding of the active material may all contribute to the prema-

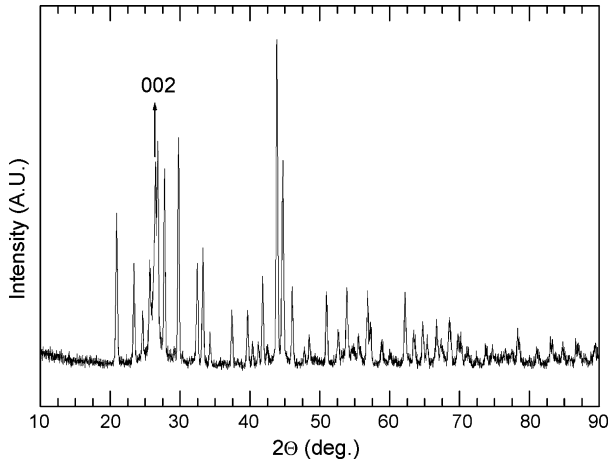

Fig. 13. X-ray diffraction pattern of graphite foam coated with lead oxide paste used as the positive electrode for a galvanostatic charge and discharge cycle between 1.0 and 2.5 V (*h k l*: graphite; unindexed: $PbSO_4$).

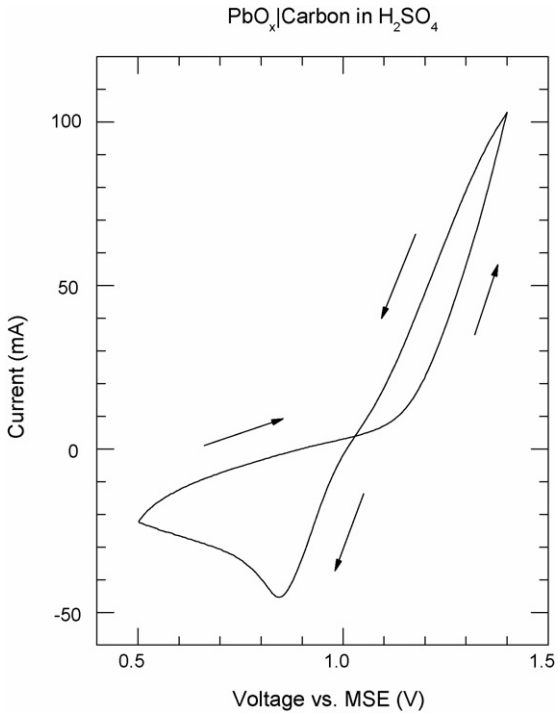

Fig. 14. Cyclic voltammogram of non-graphitized foam coated with lead oxide paste between 1.0 and 2.3 V vs. Hg/Hg_2SO_4 in saturated K_2SO_4 solution. The scan rate is 5 mV s^{-1}, and the electrolyte is 1.3 M H_2SO_4 solution.

ture capacity loss [8,21,22]. Here both of the electrodes limit the capacities. The positive electrode again limits the discharge capacity as indicated by the large voltage drop at the end of discharge. The discharge capacity is only ∼25% of the available lead for the first cycle and decreases by half for the second cycle. The possibility of formation of electrically insulating $PbSO_4$ crystals cannot be ruled out. Upon charge, the positive electrode shows an initial voltage transient, but the capacity is ultimately

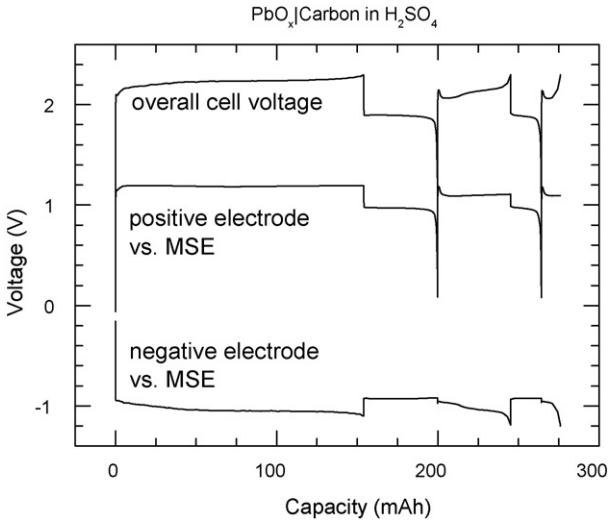

Fig. 15. Charge–discharge curves of a three-electrode cell. The positive and negative electrodes are non-graphitized foams coated with lead oxide paste, and the reference electrode is Hg/Hg_2SO_4 in saturated K_2SO_4 solution. The charge–discharge current is 10 mA, and the electrolyte is 1.3 M H_2SO_4 solution.

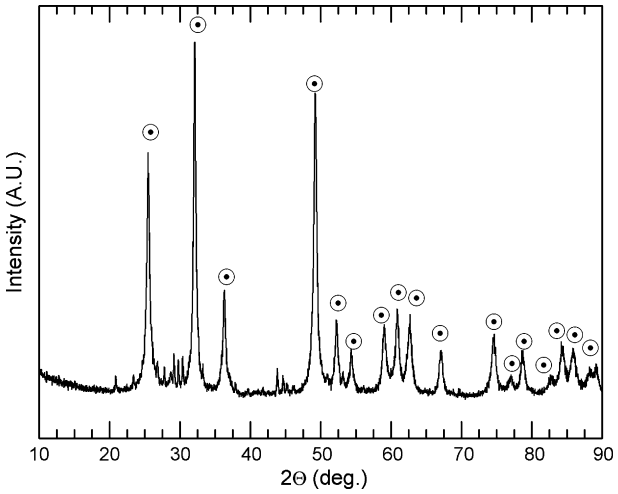

Fig. 16. X-ray diffraction pattern of non-graphitized foam coated with lead oxide paste used as the positive electrode for a galvanostatic cycling between 1.0 and 2.3 V as shown in Fig. 15 (⊙: β-PbO_2; unindexed: $PbSO_4$).

limited by polarization at the negative electrode. Further study is needed to sort out these complex effects. Optimization of the cell design, paste formulation, pasting and curing techniques, and initial charge conditions are expected to yield far better cycling performance and material utilization in the future.

4. Conclusions

Electrochemical properties of carbon foams as current collectors for lead acid batteries were characterized by cyclic voltammetry and galvanostatic charge–discharge tests. Graphite foam is electrochemically stable between −1.2 and 0 V versus Hg/Hg_2SO_4 in saturated K_2SO_4 solution. Cyclic voltammogram of graphite foam coated with lead oxide paste resembles that of metallic lead in the voltage range where the negative electrode of lead acid batteries operates. However, when used as positive current collector, intercalation of sulfuric acid into graphite occurs at 1.2 V versus Hg/Hg_2SO_4 in saturated K_2SO_4 solution. This intrinsic electrochemical instability in the voltage range where the positive electrode operates renders graphite foam not suitable for use as positive current collector for lead acid batteries. Modification of the physical and/or chemical properties is necessary to enhance the electrochemical stability in this voltage range to use graphite foams as positive current collector. Initial results indicate that the non-graphitized foams are electrochemically stable in the voltage range where the positive electrode operates. This warrants further evaluation with improved methods for mixing and applying the active electrode paste, so the cycle life and utilization can be determined. Although a great deal more work is needed, the physical properties and tunability of the physicochemical properties of graphite and non-graphtized foams make them attractive candidates for lightweight current collectors in lead acid batteries.

Acknowledgement

This research was sponsored by the Technology Transfer Program of Oak Ridge National Laboratory. Oak Ridge National Laboratory is managed by UT-Battelle, LLC for the US Department of Energy under contract DE-AC05-00OR22725.

References

[1] K. Das, A. Mondal, J. Power Sources 55 (1995) 251.
[2] A. Czerwinski, M. Zelazowska, J. Electroanal. Chem. 410 (1996) 55.
[3] A. Czerwinski, M. Zelazowska, J. Power Sources 64 (1997) 29.
[4] K. Das, A. Mondal, J. Power Sources 89 (2000) 112.
[5] E. Gyenge, J. Jung, S. Splinter, A. Snaper, J. Appl. Electrochem. 32 (2002) 287.
[6] E. Gyenge, J. Jung, B. Mahato, J. Power Sources 113 (2003) 388.
[7] J.M. Friedrich, C. Ponce-de-Leon, G.W. Reade, F.C. Walsh, J. Electroanal. Chem. 561 (2004) 203.
[8] D. Pavlov, J. Power Sources 53 (1995) 9.
[9] Power Technology, http://www.powertcbattery.com.
[10] Ultramet, UltraFoam Datasheet, http://www.ultramet.com/8.htm.
[11] J.W. Klett, US Patent No. 6,033,506 (2000).
[12] N.C. Gallego, J.W. Klett, Carbon 41 (2003) 1461.
[13] K.C. Kelley, J.J. Votoupal, US Patent Application Publication No. US 2004/0002006 A1 (2004).
[14] J.W. Klett, ORNL Graphite Foam Experimental Properties, http://www.ms.ornl.gov/researchgroups/CMT/foam/foams.htm.
[15] J.C. Duddy, F.P. Malaspina, W.J. Martini, US Patent 4,315,829 (1982).
[16] S. Fletcher, D.B. Matthews, J. Electroanal. Chem. 126 (1981) 131.
[17] A. Czerwinski, M. Zelazowska, M. Grden, K. Kuc, J.D. Milewski, A. Nowacki, G. Wojcik, M. Kopczyk, J. Power Sources 85 (2000) 49.
[18] J.O. Besenhard, E. Wudy, H. Mohwald, J.J. Nickl, W. Biberacher, W. Foag, Synth. Met. 7 (1983) 185.
[19] Y. Maeda, Y. Okemoto, M. Inagaki, J. Electrochem. Soc. 132 (1985) 2369.
[20] B.D. Cullity, Element of X-ray Diffraction, second ed., Addison-Wesley, 1978, p. 102.
[21] G. Petkova, D. Pavlov, J. Power Sources 113 (2003) 355.
[22] D. Pavlov, G. Petkova, J. Electrochem. Soc. 149 (2002) A644.